

<b>REPORT DOCUMENTATION PAGE</b>			<b>Form Approved OMB NO. 0704-0188</b>	
Public Reporting burden for this collection of information is estimated to average 1 hour per response, including the time for reviewing instructions, searching existing data sources, gathering and maintaining the data needed, and completing and reviewing the collection of information. Send comment regarding this burden estimates or any other aspect of this collection of information, including suggestions for reducing this burden, to Washington Headquarters Services, Directorate for Information Operations and Reports, 1215 Jefferson Davis Highway, Suite 1204, Arlington, VA 22202-4302, and to the Office of Management and Budget, Paperwork Reduction Project (0704-0188), Washington, DC 20503.				
1. AGENCY USE ONLY (Leave Blank)		2. REPORT DATE 3/7/07		3. REPORT TYPE AND DATES COVERED STTR FINAL REPORT, 8/8/06 - 2/8/07
4. TITLE AND SUBTITLE Development of On-Demand Non-Polar and Semi-Polar Bulk Gallium Nitride Materials for Next Generation Electronic and Optoelectronic Devices			5. FUNDING NUMBERS CONTRACT #W911NF-06-C-0133 PROJ. #R51163ST1061981	
6. AUTHOR(S) P. FINI				
7. PERFORMING ORGANIZATION NAME(S) AND ADDRESS(ES) INLUSTRATECHNOLOGIES, LLC 5385 HOLLISTER AVE. #113, SANTA BARBARA, CA 93111-2391			8. PERFORMING ORGANIZATION REPORT NUMBER	
9. SPONSORING / MONITORING AGENCY NAME(S) AND ADDRESS(ES) U. S. Army Research Office P.O. Box 12211 Research Triangle Park, NC 27709-2211			10. SPONSORING / MONITORING AGENCY REPORT NUMBER	
11. SUPPLEMENTARY NOTES The views, opinions and/or findings contained in this report are those of the author(s) and should not be construed as an official Department of the Army position, policy or decision, unless so designated by other documentation.				
12 a. DISTRIBUTION / AVAILABILITY STATEMENT Approved for public release; distribution unlimited.			12 b. DISTRIBUTION CODE	
13. ABSTRACT (Maximum 200 words)  This report was developed under STTR contract for topic "A06-T019". Inlustra Technologies and the University of California, Santa Barbara conducted a Phase I STTR research program to grow and characterize thick non-polar and semi-polar gallium nitride (GaN) wafers that will act as seeds for subsequent GaN boule growth in Phase II. Inlustra developed non-polar a-plane and m-plane GaN films with smooth surfaces and minimal wafer bowing and cracking. The growth conditions for each crystallographic plane were primarily optimized with respect to surface morphology. Defect reduction methods were then applied to achieve low average extended defect density across the seed wafers. UCSB researchers conducted detailed microstructural characterization on these non-polar and semi-polar GaN thick films to evaluate their utility as seeds for equiaxed GaN boule growth in Phase II.				
14. SUBJECT TERMS STTR Final Report			15. NUMBER OF PAGES 17	
			16. PRICE CODE	
17. SECURITY CLASSIFICATION OR REPORT UNCLASSIFIED	18. SECURITY CLASSIFICATION ON THIS PAGE UNCLASSIFIED	19. SECURITY CLASSIFICATION OF ABSTRACT UNCLASSIFIED	20. LIMITATION OF ABSTRACT UL	

NSN 7540-01-280-5500

Standard Form 298 (Rev.2-89)  
Prescribed by ANSI Std. Z39-18  
298-102

Enclosure 1

**TABLE OF CONTENTS**

**LIST OF FIGURES ..... iii**

**PHASE I OBJECTIVES ..... 1**

**SUMMARY OF PHASE I WORK..... 2**

**REFERENCES..... 17**

## LIST OF FIGURES

	Page
Fig. 1. Nomarski optical contrast micrograph of: (a) a relatively smooth <i>m</i> -plane GaN film growth on a LiAlO <sub>2</sub> substrate; (b) a rougher <i>m</i> -plane GaN film growth on a LiAlO <sub>2</sub> substrate, and (c) a very smooth <i>m</i> -plane GaN film grown on a LiAlO <sub>2</sub> substrates with optimized growth parameters to reduce grown-in stress.	2
Fig. 2. SIMS depth profiles of <i>m</i> -plane GaN films grown on LiAlO <sub>2</sub> substrates: (a) Comparison of the hydrogen and lithium concentrations at the front and back surfaces of a 120 μm-thick GaN film. (b) Comparison of two GaN films having quite different Li and H concentrations. The growth parameters and film thicknesses of these two films were identical, with only the ramp conditions having been altered.	3
Fig. 3. (a) 5 x 5 μm AFM micrograph of a 45 μm thick <i>m</i> -plane GaN film. The RMS roughness of the film is approximately 0.64 nm. (b) 5 x 5 μm atomic force micrograph of a 335 μm thick <i>m</i> -plane GaN film, with an RMS roughness of 1.9 nm.	4
Fig. 4. Nomarski optical contrast micrograph of an <i>a</i> -plane GaN film grown on a 53 mm diameter <i>r</i> -plane sapphire substrate. The cracks visible in the image were sub-surface and healed during growth.	5
Fig. 5. Atomic force micrograph (4 x 5 μm) of an <i>a</i> -plane GaN film surface. Comparable roughness of ~ 1 nm was observed across the entire 2" diameter of the film.	5
Fig. 6. Cross-sectional schematic of the Double LEO process for non-polar GaN films. (a) an SiO <sub>2</sub> mask is deposited on a smooth template, and is selectively etched to form stripes; (b) the first LEO re-growth is carried out to coalescence; (c) the coalesced LEO film is coated with a second mask which is offset from the first by approximately half a period; (d) the second LEO re-growth is carried out to coalescence.	6
Fig. 7. (a). SEM image of LEO stripes grown from a patterned LiAlO <sub>2</sub> substrate; (b) Digital photograph revealing polishing damage in a thermally-etched and cycled LiAlO <sub>2</sub> substrate.	6
Fig. 8. Nomarski optical contrast micrographs of: (a) coalesced <i>m</i> -plane GaN LEO stripes oriented along the <0001>-direction; (b) coalesced <i>m</i> -plane GaN LEO stripes oriented along the <11 $\bar{2}$ 0>-direction; (c) coalesced but rough <i>m</i> -plane GaN LEO stripes oriented along the <11 $\bar{2}$ 0>-direction; (d) cracking in coalesced <i>m</i> -plane LEO GaN on a SiC substrate.	8
Fig. 9. Nomarski optical contrast micrograph of coalesced <i>a</i> -plane GaN LEO stripes (oriented horizontally). The lines running top-to-bottom are gradual surface undulations with a peak-to-valley height of < 150 nm.	9
Fig. 10. (a) <i>a</i> -plane LEO SEM cross-section of un-coalesced stripes; (b) cross-section of coalesced stripes (visible features are cleaving artifacts). Both cross sections look along the <i>m</i> -direction <1 $\bar{1}$ 00>.	10

Fig. 11. 10 x 10 $\mu\text{m}$ $a$ -plane LEO AFM comparing a Ga-face wing (left side) to window (right side). The RMS roughness was 0.4 nm on the wing, compared to 1.1 nm on the window.	10
Fig. 12. Schematic of the S-LEO process, in which a GaN film is selectively masked and etched to yield periodic trenches. Re-growth occurs in such a way that nearly all extended defects are blocked in one growth run. Courtesy of B. Imer.	11
Fig. 13. Cross-sectional SEM images of sidewall-LEO films. (a) sidewall nucleation stage; (b) planar pillar lateral growth; and (c) cross-section of coalesced film (surface features are cleaving artifacts).	12
Fig. 14. 25x25 $\mu\text{m}$ AFM scan of a coalesced $a$ -plane S-LEO film. Vertical lines visible in "N-Face Lateral Growth" region are stacking faults.	12
Fig. 15. Inclined SEM cross-section micrographs of $\langle 1\bar{1}01 \rangle$ -oriented $a$ -plane LEO stripes before (top) and after (bottom) coalescence.	13

## PHASE I OBJECTIVES

The primary technical objective of Inlustra's Phase I STTR project was the HVPE growth of thick, free-standing **non-polar** GaN wafers of 2-inch diameter, which would be appropriate as high-quality seeds for subsequent equiaxed GaN boule growth. Specifically, the goals of this project were:

**(a) Development of smooth, planar non-polar and semi-polar GaN films as templates for Double LEO**

The first stage in the project focused on the reproducible HVPE film growth of smooth, planar non-polar *a*- and *m*-plane GaN films, with some initial studies concerning semi-polar {10 $\bar{1}$ 1} and {10 $\bar{1}$ 3} films. All types of films were to be grown on substrates of two-inch diameter. Research was needed to better understand the dependence of surface morphology on varying HVPE growth conditions such as temperature and precursor gas flows. Two-inch diameter *a*-plane GaN films were to be grown on *r*-plane sapphire, and *m*-plane films were to be grown on lithium aluminate (LiAlO<sub>2</sub>) or *m*-plane silicon carbide (SiC). While non-polar substrate development was to be the primary focus of the Phase I project, time permitting semi-polar film and substrate growth would also be explored. Based on previous results at the University of California, Santa Barbara (UCSB), two-inch diameter semi-polar {10 $\bar{1}$ 1} films were to be grown on (100) spinel substrates, and {10 $\bar{1}$ 3} films were to be grown on (110) spinel or *m*-plane {10 $\bar{1}$ 0} sapphire substrates.

**(b) Double LEO for uniform extended defect reduction**

Research by Inlustra personnel while at UCSB showed that single-step lateral epitaxial overgrowth (LEO) is effective at locally reducing the areal density of extended defects in non-polar *a*- and *m*-plane films. In Phase I, when feasible the LEO process was utilized in a repeated fashion: a periodically stripe-patterned mask would be overgrown with GaN such that a planar coalesced surface would be obtained; then a second offset mask would be deposited and overgrown such that regions where defects had vertically propagated were now blocked by the second mask. This approach to defect reduction, though initially time-consuming, was expected to result in thick non-polar and semi-polar seed GaN films containing a uniformly low extended defect density of  $5 \times 10^6 \text{ cm}^{-2}$  or less.

**(c) Detailed structural, optical and electrical characterization of epitaxial films and free-standing wafers**

Throughout Phase I non-polar and semi-polar GaN growth development, detailed structural characterization was to be carried out by both Inlustra and UCSB personnel as continuous feedback for HVPE crystal growth optimization. Such rapid characterization was readily available using UCSB recharge facilities, in the form of atomic force microscopy, X-ray diffractometry, and scanning electron microscopy equipment, among others. These techniques provided quantitative and semi-quantitative information about atomic-scale film surface morphology, extended defect levels (structural mosaic), and micron-scale cross-sectional imaging (*e.g.* useful for LEO development). Optical characterization (photoluminescence) and electrical measurements (Hall Effect) were to be occasionally used when relevant to HVPE GaN film growth development.

## SUMMARY OF PHASE I WORK

Inlustra's Phase I STTR research focused predominantly on the growth of thick non-polar *m*-plane and *a*-plane gallium nitride (GaN) films by hydride vapor phase epitaxy (HVPE). This vapor-phase crystal growth technique is widely viewed in the GaN industry as the most direct, economical means of obtaining sizeable (~ 2-inch diameter) GaN substrates, since the growth rate can exceed 100  $\mu\text{m/hr}$ , possibly without sacrificing crystal quality. Inlustra's Phase I non-polar GaN growth research utilized a research-scale HVPE growth system, which limited the duration of growth runs, and therefore the ultimate non-polar GaN film thickness that could be achieved. We are now bringing a true production-scale GaN crystal growth system on-line, which will be capable of the extended growth duration needed for equiaxed boule growth.

### *m*-plane GaN films

Initially, HVPE growth parameters were refined for growth of thick free-standing *m*-plane GaN films on (100)  $\text{LiAlO}_2$  substrates. Flat, free-standing *m*-plane films with thicknesses up to ~ 1000  $\mu\text{m}$  (1 mm) were produced, with the benefit of self-separation of the GaN films from their  $\text{LiAlO}_2$  substrates upon cool-down from growth. Morphological characterization of these films at UCSB was directed on surface morphology, using the high-resolution technique of atomic force microscopy (AFM). Inlustra personnel first screened *m*-plane GaN films using Nomarski optical contrast microscopy, which revealed surface roughness of a more macroscopic nature. As shown in Fig. 1, this interference-based method highlights roughness that would otherwise be difficult to observe in an optical microscope.

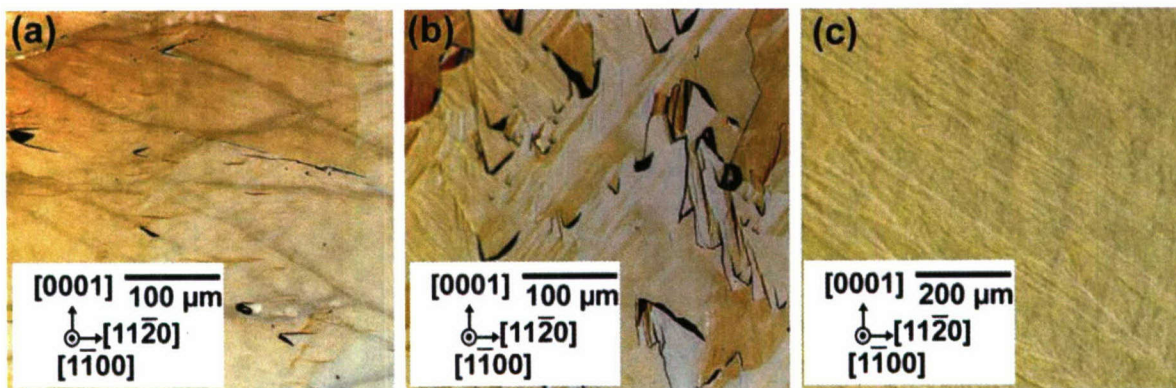


Fig. 1. Nomarski optical contrast micrograph of: (a) a relatively smooth *m*-plane GaN film growth on a  $\text{LiAlO}_2$  substrate; (b) a rougher *m*-plane GaN film growth on a  $\text{LiAlO}_2$  substrate, and (c) a very smooth *m*-plane GaN film grown on a  $\text{LiAlO}_2$  substrates with optimized growth parameters to reduce grown-in stress.

Radii of curvature of the as-grown films, and indicator of residual stress level, was measured by X-ray diffraction and/or multiple optical beam reflectance measurements<sup>1</sup>. At the beginning of the growth study, films having smoother surfaces (*e.g.* Fig. 1(a)) typically exhibited small radii of curvature (*i.e.* higher residual stress), whereas rough films (Fig. 1(b)) had comparatively large radii of curvature (and thus lower residual stress). This roughness-stress correlation has been commonly observed in the film growth of other materials systems, since the additional surface area created by the roughness partially accommodates in-grown stress. With subsequent HVPE growth development we were able to reduce the tendency of smoother *m*-plane films to

have higher stress. Particular attention was given to the initial film growth conditions (e.g. V/III ratio and growth rate within the first few minutes), since they appeared to strongly influence the GaN-LiAlO<sub>2</sub> interfacial bonding strength, and thus the amount of in-grown stress.

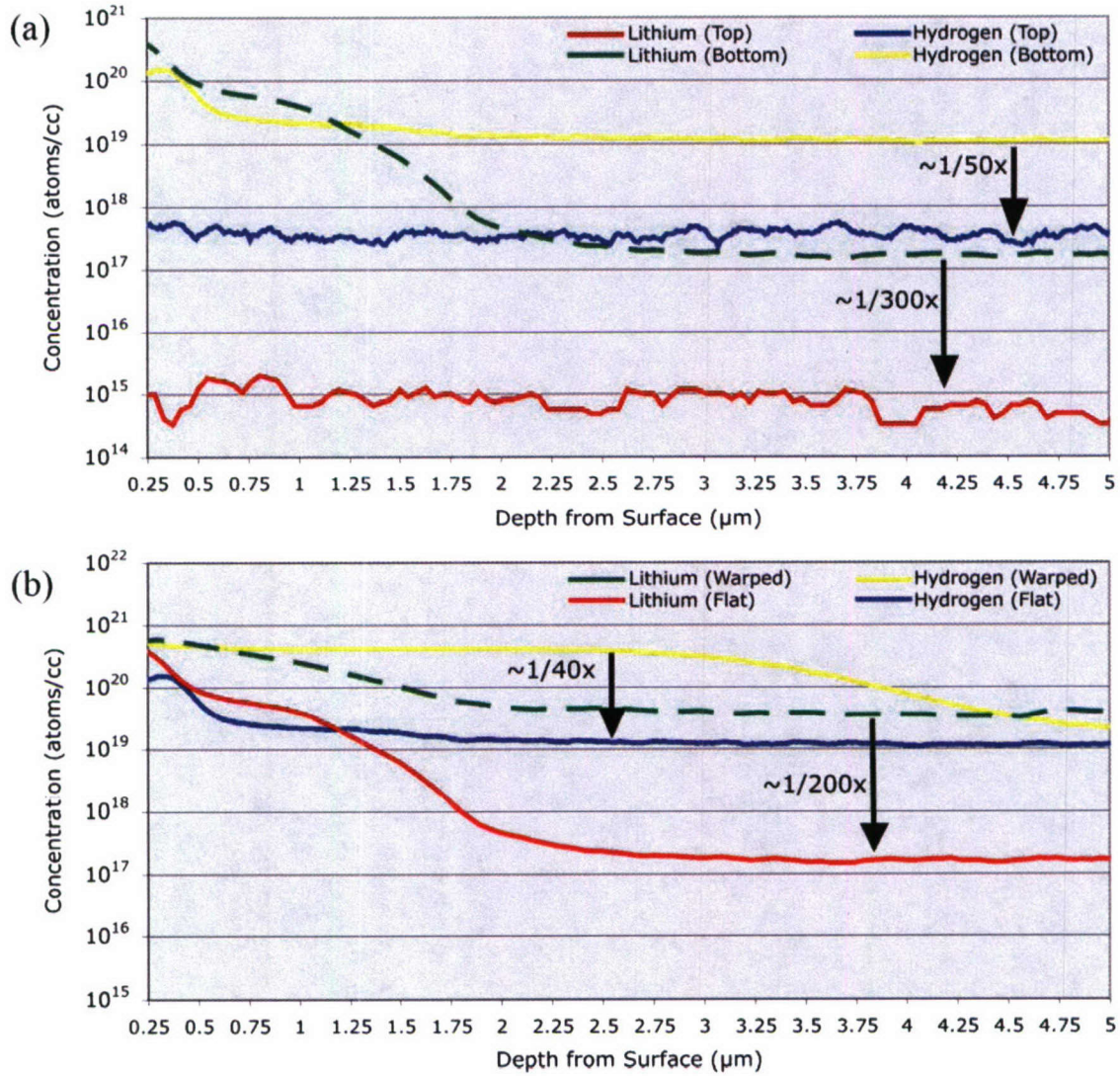


Fig. 2 SIMS depth profiles of *m*-plane GaN films grown on LiAlO<sub>2</sub> substrates: (a) Comparison of the hydrogen and lithium concentrations at the front and back surfaces of a 120 μm-thick GaN film. (b) Comparison of two GaN films having quite different Li and H concentrations. The growth parameters and film thicknesses of these two films were identical, with only the ramp conditions having been altered.

HVPE pre-growth ramp conditions were also refined, since the gas composition prior to GaN growth strongly influenced the tendency for the LiAlO<sub>2</sub> substrate to decompose during heating to the growth temperature. As the decomposition rate of the substrate increased, so did impurity incorporation into the back side of the GaN film, causing significant stress due to impurity concentration gradients from the bottom to the top of the GaN films. Secondary Ion Mass Spectroscopy (SIMS) analysis of the front and back surfaces of GaN films grown by HVPE demonstrated that the hydrogen and lithium concentrations in the first two micrometers of GaN

from each surface were 100-10,000 times higher on the surface in contact with the LiAlO<sub>2</sub> substrate than at the free surface following growth (see Fig. 2(a)). Indeed, substrate decomposition control appears to be vital to managing wafer curvature. Figure 2 (b) shows SIMS plots of hydrogen and lithium concentrations for two GaN films. The film containing the higher Li and H concentrations curled excessively during cooling to exhibit an unusually small radius of curvature of less than 1 cm. In contrast, adjusting the pre-growth ramp parameters to decrease LiAlO<sub>2</sub> decomposition yielded a >100-fold drop in Li and H concentrations at a depth of three  $\mu\text{m}$  from the back surface of the GaN film. The resulting free-standing GaN film was essentially flat with a radius of curvature in excess of 10 m.

The *m*-plane GaN films with few visible surface features in Nomarski microscopy were then characterized using AFM, with typical film surfaces shown in Fig. 3. Surfaces of thicker films (*e.g.* > 335  $\mu\text{m}$ ) initially tended to be rougher, as shown in Fig. 3(b) (as opposed to the smoother surfaces shown in Fig. 3(a)). Using root-mean-square (RMS) roughness calculations from AFM scans as an indicator, we studied the causes of this phenomenon, which appeared to again be due to stress-induced roughening. Adjustment of HVPE growth parameters was largely successful at mitigating the onset of surface roughness with increasing thickness; studies to validate this conclusion are ongoing during the Interim Work Period. We are now investigating the use of HVPE growth parameter variation (continuously or in steps) over the course of a given thick-film *m*-plane GaN growth to accommodate/control changes in surface morphology.

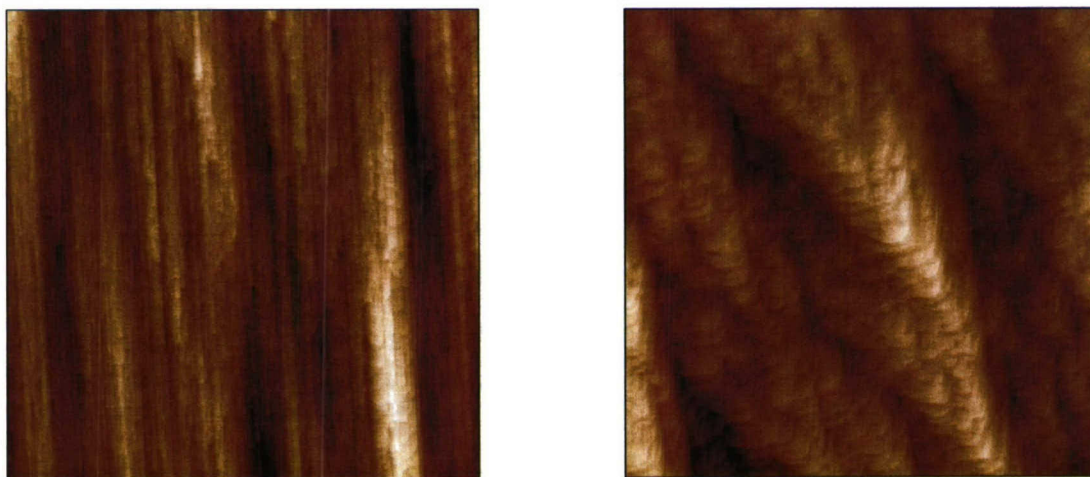


Fig. 3. (a) 5 x 5  $\mu\text{m}$  AFM micrograph of a 45  $\mu\text{m}$  thick *m*-plane GaN film. The RMS roughness of the film is approximately 0.64 nm. (b) 5 x 5  $\mu\text{m}$  atomic force micrograph of a 335  $\mu\text{m}$  thick *m*-plane GaN film, with an RMS roughness of 1.9 nm.

### *a*-plane GaN films

Subsequent HVPE growth experiments shifted to the growth of *a*-plane GaN films on *r*-plane sapphire substrates. The investigators' previous experience at UCSB showed that *a*-plane GaN films grown directly on sapphire tended to roughen significantly when the growth parameters were not tightly controlled due to the presence of a high density of microstructural defects. Thus during Phase I research we studied the dependence of *a*-plane GaN film surface morphology on key parameters such as temperature, ammonia (NH<sub>3</sub>) flow, and growth rate (primarily controlled by HCl flow rate over metallic Gallium to form GaCl<sub>x</sub>). A particular emphasis was placed on utilizing films grown on 53 mm diameter sapphire substrates, thereby yielding two-inch diameter

uniform GaN films after edge exclusion from the wafer holder in the HVPE growth chamber. Uniform  $a$ -plane GaN films were successfully deposited over this large area, yielding  $a$ -plane ‘template’ films for subsequent thick film growth and/or processing for defect reduction via lateral epitaxial overgrowth (see below). Ultimately, growth rate variation of less than  $\sim 5\%$  was achieved across a 2-inch wafer diameter, which contributed to proper control of stress (and therefore bowing) in the as-grown wafers.

Figure 4 below shows a Nomarski optical contrast micrograph of a representative  $a$ -plane GaN film. Long-range striations/undulations were often observed, which were of approximately 100 nm in peak-to-valley height. The origin of such striations is unclear at present, but they are not believed to be detrimental to subsequent lithographic patterning for defect reduction due to their large lateral extents. As previously observed by Haskell *et al.* at UCSB, any cracks that developed during growth due to grain coalescence stresses subsequently ‘healed’ via lateral growth, and indeed acted as a mode of relief for stress that developed from the lattice mismatch between the  $a$ -plane GaN film and its underlying sapphire substrate. Figure 5 shows an AFM scan of the film in Fig. 4, demonstrating the low surface roughness achieved through HVPE growth parameter optimization. Here we focused on the interplay between  $\text{NH}_3$  and gallium chloride ( $\text{GaCl}_x$ ) flows in the HVPE chamber, since the tendency of thick  $a$ -plane films to roughen appeared to be particularly sensitive to the ratio of these flows.

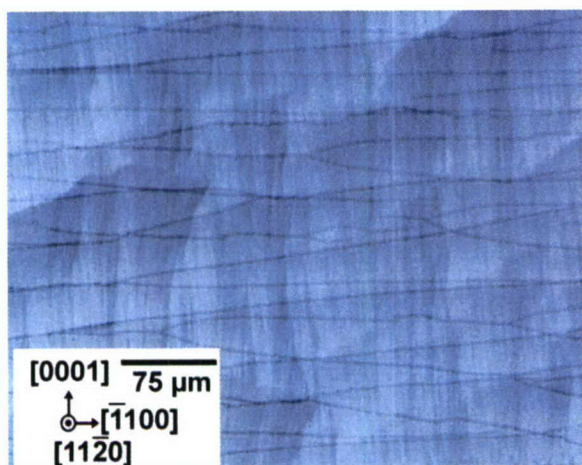


Fig. 4. Nomarski optical contrast micrograph of an  $a$ -plane GaN film grown on a 53 mm diameter  $r$ -plane sapphire substrate. The cracks visible in the image were sub-surface and healed during growth.

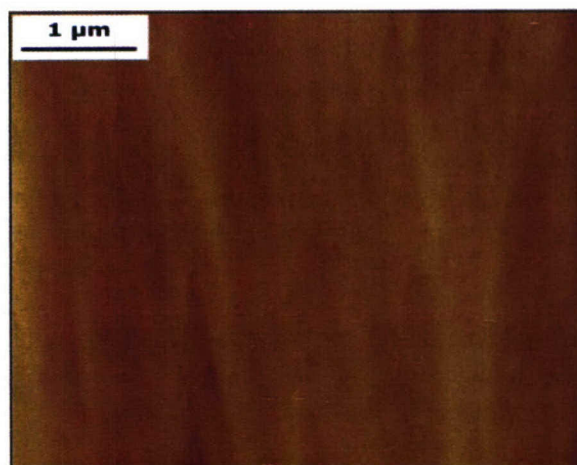


Fig. 5. Atomic force micrograph ( $4 \times 5 \mu\text{m}$ ) of an  $a$ -plane GaN film surface. Comparable roughness of  $\sim 1 \text{ nm}$  was observed across the entire 2" diameter of the film.

### LEO for Defect Reduction

The principal ongoing challenge during  $m$ -plane and  $a$ -plane GaN direct growth studies was the management of microscopic defects such as threading dislocations (TDs) and stacking faults (SFs) that arose due to film-substrate lattice mismatch and other factors. Threading dislocations, often present in an areal density of  $> 1 \times 10^9 \text{ cm}^{-2}$ , are generally known to be non-radiative recombination centers and leakage pathways in  $c$ -plane GaN. For lasers in particular, device lifetime is adversely affected by the presence of TDs, and the same can be assumed for corresponding non-polar GaN devices. It is not yet known whether SFs in non-polar GaN films

are likewise deleterious to device efficiency, but their associated partial dislocations are likely harmful.

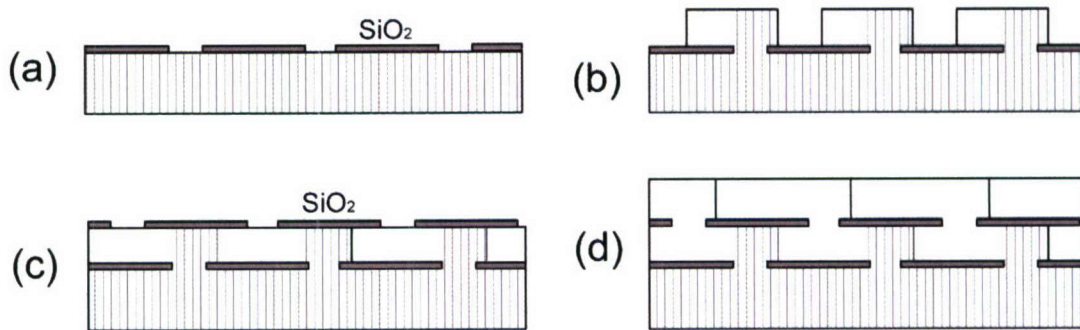


Fig. 6. Cross-sectional schematic of the Double LEO process for non-polar GaN films. (a) an  $\text{SiO}_2$  mask is deposited on a smooth template, and is selectively etched to form stripes; (b) the first LEO re-growth is carried out to coalescence; (c) the coalesced LEO film is coated with a second mask which is offset from the first by approximately half a period; (d) the second LEO re-growth is carried out to coalescence.

The most direct means of lowering dislocation density in non-polar GaN is lateral epitaxial overgrowth (LEO), since the density of TD and SFs does not readily decrease by simply growing thick films, as in the case of *c*-plane GaN,. In the LEO technique, a film is coated with a mask that has been periodically etched (typically in a stripe pattern) to leave exposed film areas. Re-grown GaN selectively deposits in the open areas ('windows') and overgrows the mask ('wings'), thereby blocking the vertical propagation of dislocations and stacking faults. This is shown schematically in Fig. 6, which depicts Double LEO, *i.e.* two LEO patterning and re-growth cycles for 'complete' removal of TDs and SFs at the film surface.

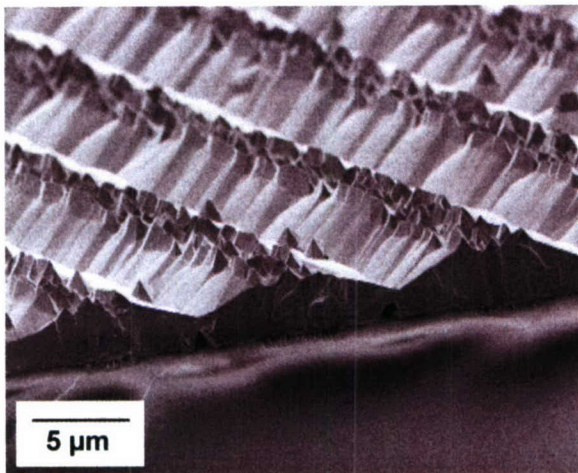


Fig. 7(a). SEM image of LEO stripes grown from a patterned  $\text{LiAlO}_2$  substrate.

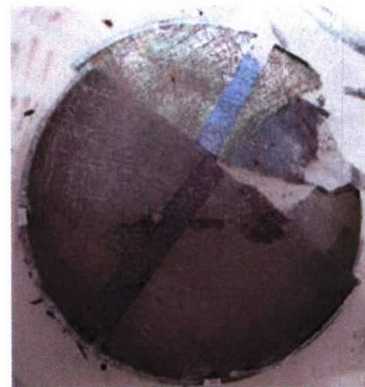


Fig. 7(b). Digital photograph revealing polishing damage in a thermally-etched and cycled  $\text{LiAlO}_2$  substrate.

The majority of the *m*-plane GaN-related work performed in Phase I focused on growth of thick, planar, free-standing GaN films regardless of the defect content of those films. This approach was driven by several observations:

- LEO cannot be performed directly on LiAlO<sub>2</sub> substrates due to chemical attack of the substrate in the photolithographic processing steps. See Fig. 7(a) for an example of stripe morphology when taking this approach.
- Molecular beam epitaxy (MBE) can be used to first deposit thin *m*-plane GaN templates on the LiAlO<sub>2</sub> substrates. These templates could then be used for LEO processing. Chemical attack remained a problem, but thermal cycling of the substrate caused thermal etching of the LiAlO<sub>2</sub> and exposure of polishing damage in the substrate. LEO films grown by this approach tended to be very inhomogeneous. Fig. 7(b) shows an example of such a LiAlO<sub>2</sub> substrate with polishing damage highlighted by cyclical thermal etching.
- *m*-plane LEO can be performed using *m*-plane GaN/AlN templates first grown by MBE on *m*-plane 4H- or 6H-SiC substrates. Coalescence of <0001>-oriented stripes is readily achieved over large areas (nearly 100% of a wafer's surface area) as is shown in Fig. 8(a), but both TDs and SFs persist in the film when using this stripe orientation. Coalescence of <11 $\bar{2}$ 0> stripes has been achieved as well, as shown in Fig. 8(b), but with a lower success rate (~25%) and much poorer uniformity (planar coalescence is often confined to <20% of the surface area). Uneven steps are often observed on the surface at the coalescence fronts, as shown in Fig. 8(c). However, this stripe orientation does provide for the elimination of both TDs and SFs in the Ga-terminated wings.
- Thermal expansion mismatch-related cracking is problematic for *m*-plane GaN LEO when performed on *m*-plane SiC substrates, an example of which is shown in Fig. 8 (d). Unlike in *a*-plane GaN growth on *r*-plane Al<sub>2</sub>O<sub>3</sub>, in which cracks that form during growth tend to heal via lateral growth, these cracks in *m*-plane GaN LEO films form during cooling rather than growth, and therefore cannot heal.

Based on the above results, we believe the most practical approach to achieving reproducible *m*-plane GaN LEO is to first produce thick, free-standing *m*-plane GaN films, then perform LEO on them, thus eliminating the strong influences of chemical attack and thermal expansion mismatch that are inherent to growth on foreign substrates. However, we have continued to improve our understanding of *m*-plane GaN LEO by utilizing *m*-plane SiC substrates. We expect the growth parameters developed in this process to port readily to LEO on free-standing GaN substrates. The LEO process consisted of the following steps:

- deposition of an MBE-grown AlN nucleation layer and ~500 nm of GaN on an *m*-plane SiC substrate.
- deposition of an SiO<sub>2</sub> mask on the *m*-plane GaN template, using PECVD primarily.
- lithographic patterning of the SiO<sub>2</sub> layer with periodic stripe patterns consisting of 2-3  $\mu$ m wide openings and 7-8  $\mu$ m wide stripes.
- wet etching in an aqueous 10% HF solution to remove the SiO<sub>2</sub> from the narrow window regions.
- removal of photoresist, sample cleaning, and inspection of the mask.

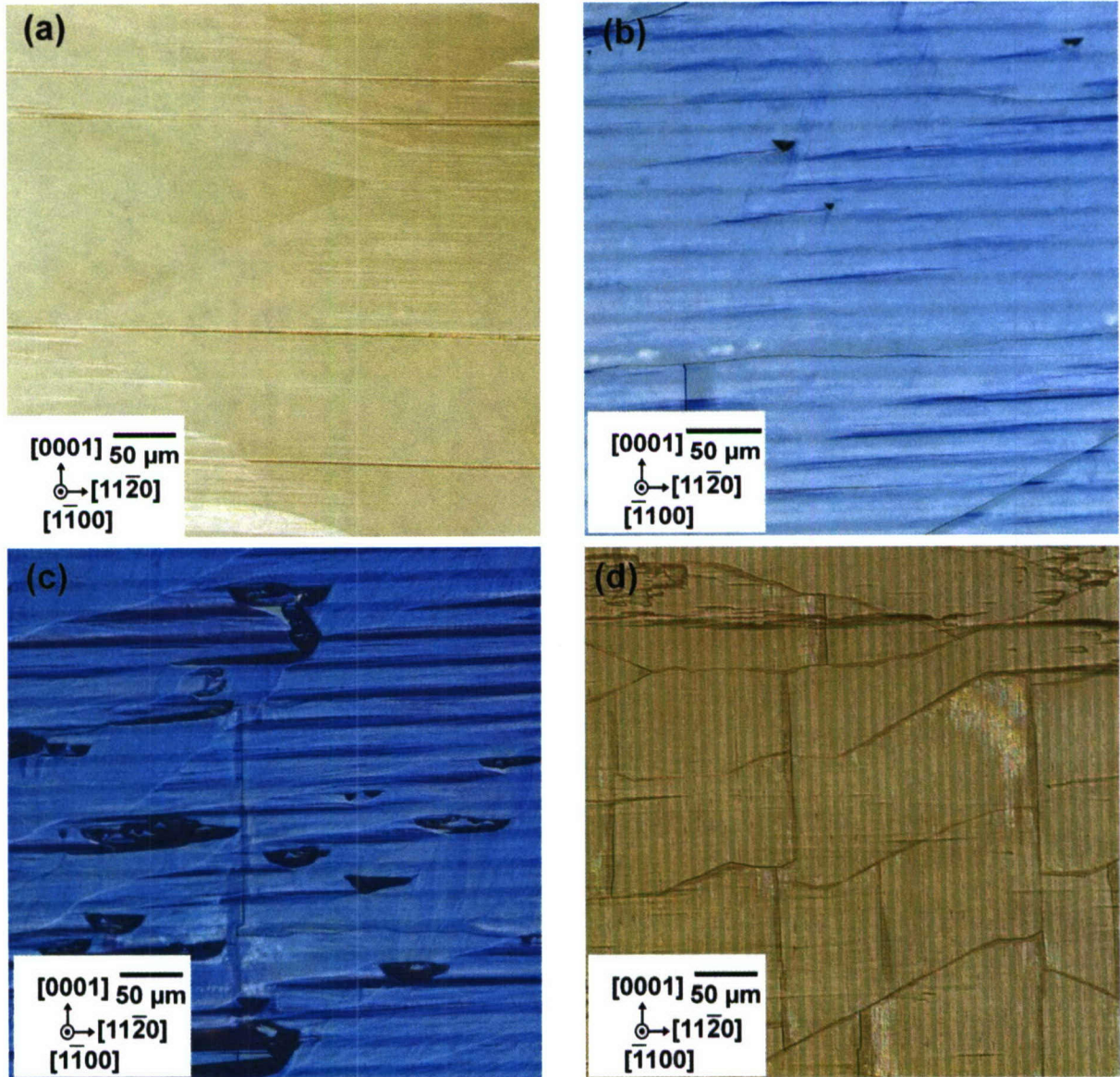


Fig. 8. Nomarski optical contrast micrographs of: (a) coalesced *m*-plane GaN LEO stripes oriented along the  $\langle 0001 \rangle$ -direction; (b) coalesced *m*-plane GaN LEO stripes oriented along the  $\langle 11\bar{2}0 \rangle$ -direction; (c) coalesced but rough *m*-plane GaN LEO stripes oriented along the  $\langle 11\bar{2}0 \rangle$ -direction; (d) cracking in coalesced *m*-plane LEO GaN on a SiC substrate.

The LEO re-growth parameters we utilized built upon the work of Haskell *et al.* at UCSB, primarily by refining growth parameters to increase uniformity and reproducibility of *m*-plane LEO stripe growth and coalescence. By the close of the Phase I effort, we had better defined the range of V/III ratios and growth temperatures that yielded more consistent *m*-plane LEO results, though additional improvement is of course still required.

During Phase I, LEO studies were primarily performed on *a*-plane GaN films, which were typically more mechanically robust (when still in contact with their host sapphire substrates) than free-standing *m*-plane GaN films of the same thickness. LEO processing in this case consisted of:

- deposition of an SiO<sub>2</sub> mask on the *a*-plane film, using PECVD or e-beam deposition
- lithographic patterning and development of an overlying photoresist with a periodic stripe pattern (either 2 μm wide stripes with 8 μm between them, and 5 μm wide stripes with 15 to 55 μm in between)
- wet etching (with dilute HF solution) or dry etching (with SF<sub>6</sub> RIE) to etch exposed SiO<sub>2</sub> areas
- removal of remaining photoresist, including 'de-scum' in O<sub>2</sub> plasma
- Nomarski optical microscopy inspection of etched SiO<sub>2</sub> mask to verify complete etch

Once lithographic processing was complete, the wafer was returned to the HVPE growth chamber for LEO. Building on initial findings by Haskell *et al.* at UCSB, *a*-plane LEO regrowth was conducted with an emphasis on obtaining smooth coalescence (merging of neighboring LEO stripes). Stripe-stripe coalescence was fairly uniform across the two-inch wafer, an example of which is shown in Figs. 9 and 10 below. It became evident that proper control of HVPE growth conditions enabled large Ga-face 'wing' (overgrown) regions to reproducibly develop, in which the residual dislocation and stacking fault densities were quite low ( $< 1 \times 10^6 \text{ cm}^{-2}$  and  $< 1 \times 10^3 \text{ cm}^{-1}$ , respectively). Meanwhile, N-face wings, which had low TD density but still contained fairly high SF density, were quite narrow. Unlike the case for *m*-plane LEO, the ratio of Ga- to N-face wing lateral growth for *a*-plane GaN LEO stripes was typically more than 6:1. Given sufficient surface smoothness and large Ga-terminated wings, such coalesced LEO films could then be patterned again with a selectively etched mask which is offset from the first mask, and the LEO growth process repeated.

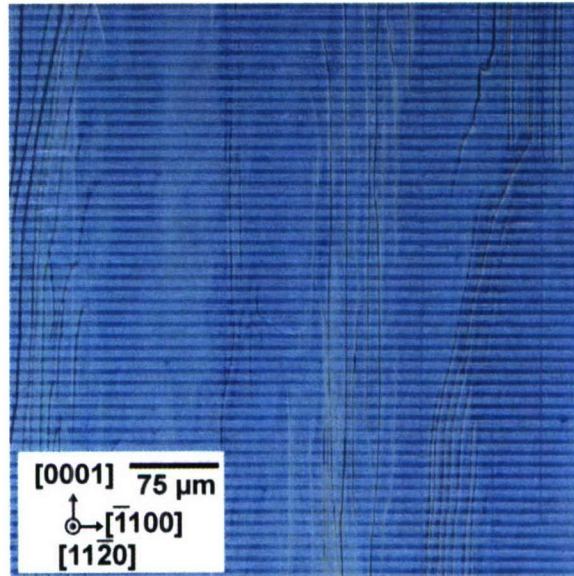


Fig. 9. Nomarski optical contrast micrograph of coalesced *a*-plane GaN LEO stripes (oriented horizontally). The lines running top-to-bottom are gradual surface undulations with a peak-to-valley height of  $< 150 \text{ nm}$ .

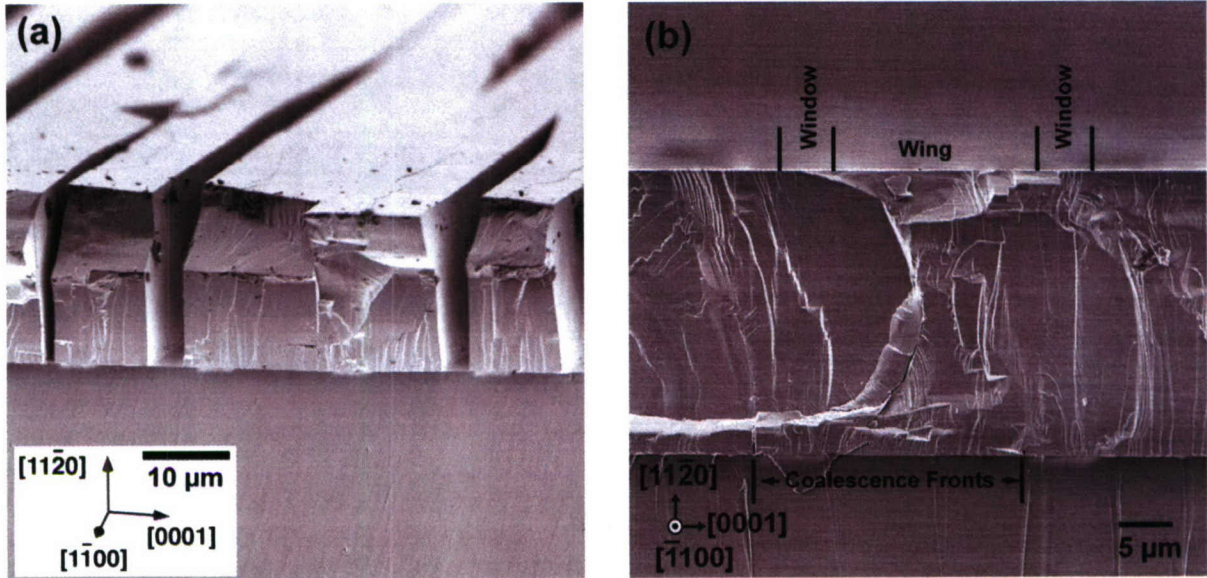
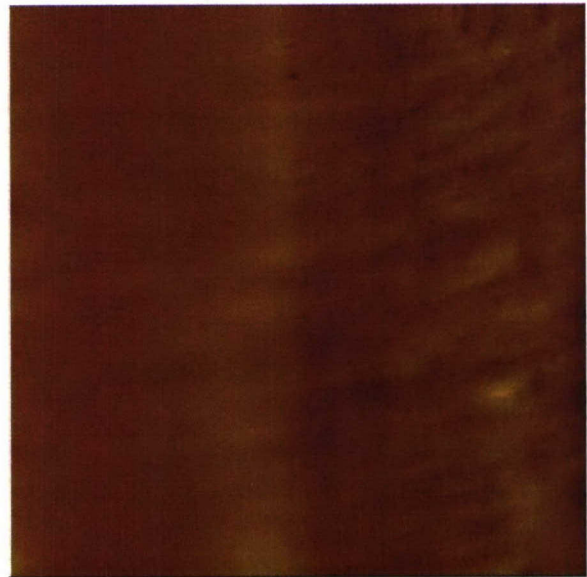


Fig. 10. (a)  $\alpha$ -plane LEO SEM cross-section of un-coalesced stripes; (b) cross-section of coalesced stripes (visible features are cleaving artifacts). Both cross sections look along the  $m$ -direction  $\langle 1100 \rangle$ .

AFM measurements were routinely used to evaluate the effectiveness of LEO defect reduction, and also verify that smooth surface morphology was maintained, as shown in Fig. 11. An encouraging aspect of TD and SF reduction in the wings was that their surfaces became correspondingly smoother. As described above, the typical RMS roughness of planar  $\alpha$ -plane GaN films examined during this project ranged from  $\sim 0.8$  nm to  $\sim 1.6$  nm. LEO processing with stripes oriented along the  $[1100]$  direction yielded surfaces with RMS roughness routinely below 0.5 nm over a comparable area. As we view low surface roughness of the seed film as a critical parameter in maintaining subsequent high-quality GaN boule growth for extended periods, the roughness reduction achieved via LEO is encouraging.

Fig. 11.  $10 \times 10 \mu\text{m}$   $\alpha$ -plane LEO AFM comparing a Ga-face wing (left side) to window (right side). The RMS roughness was 0.4 nm on the wing, compared to 1.1 nm on the window.



### ***Sidewall LEO (S-LEO)***

Although the D-LEO approach is relatively straightforward, it requires two sets of lithography and re-growth steps, and is therefore time- and labor-intensive. Difficulties are frequently encountered in properly offsetting the stripe openings in the second mask level with those of the first. Not only must the windows in the second level be parallel to those in the first level, but they must be located so as to avoid the N-face wing and the stripe-stripe coalescence fronts in the first layer, neither of which can be conveniently observed in an optical aligner. In addition, smooth coalescence of the first LEO step must be achieved in order to uniformly deposit and etch the second patterned mask. Any flaws in one of these serial steps will be carried through the process such that the second LEO coalesced surface will have macroscopic defects such as pits, cracks, or inclusions. Initial experiments with double LEO suggested its feasibility but appeared unlikely to yield a robust, cost-effective process for manufacturing of non-polar GaN seed films. Therefore, we set upon a variation of conventional LEO, called sidewall LEO, as a means of obtaining uniform defect reduction in a single re-growth step. Sidewall LEO (S-LEO) was first demonstrated at UCSB for defect reduction in MOCVD-grown *a*-plane films.<sup>2</sup> A schematic of this process is shown in Fig. 12, in which initial re-growth occurs laterally from the sidewalls of mesas or trenches instead of vertically through mask openings.

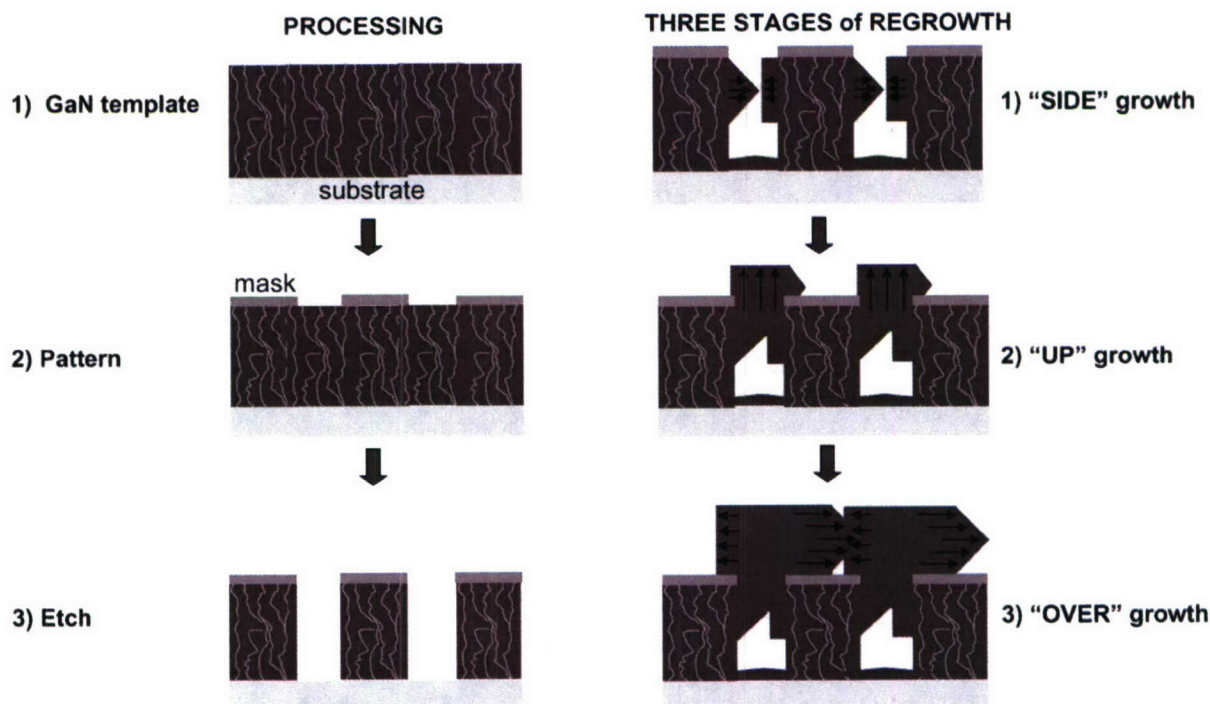


Fig. 12. Schematic of the S-LEO process, in which a GaN film is selectively masked and etched to yield periodic trenches. Re-growth occurs in such a way that nearly all extended defects are blocked in one growth run. Courtesy of B. Imer.

We adapted the S-LEO process to HVPE *a*-plane GaN growth, and achieved some very promising initial results. Trenches were etched in a thick *a*-plane GaN film on *r*-plane sapphire, and SiO<sub>2</sub> was deposited on the tops and N-face sidewalls of the resulting mesas to block re-growth in these areas. Figure 13 provides a series of cross-sectional SEM images from S-LEO

samples showing the evolution from initial sidewall nucleation to planarization and ultimately coalescence. Ultimate template thicknesses grown using the S-LEO approach tended to be thicker (50-75  $\mu\text{m}$ ) than would be performed for a D-LEO process (two layers of 10-15  $\mu\text{m}$  each), but because the S-LEO process utilizes only a single defect reduction step, the process is much less time-intensive than D-LEO.

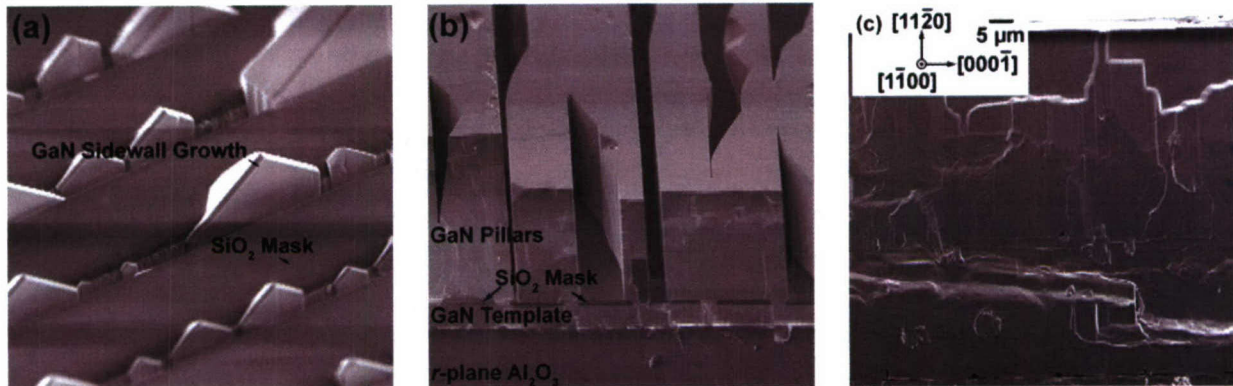


Fig. 13. Cross-sectional SEM images of sidewall-LEO films. (a) sidewall nucleation stage; (b) planar pillar lateral growth; and (c) cross-section of coalesced film (surface features are cleaving artifacts).

Using the same growth conditions as those for standard  $a$ -plane LEO, the re-growth morphology in Fig. 14 was obtained, which resulted from stable lateral/vertical growth, followed by stripe-stripe coalescence. Smooth coalescence was achieved over  $\sim 90\%$  of the 2-inch wafer, resulting in uniform defect reduction. As measured in AFM and confirmed with TEM (not shown), a threading dislocation density value of  $< 2 \times 10^6 \text{ cm}^{-2}$  was achieved. Thus the feasibility of S-LEO for uniform defect reduction in a single re-growth step was demonstrated.

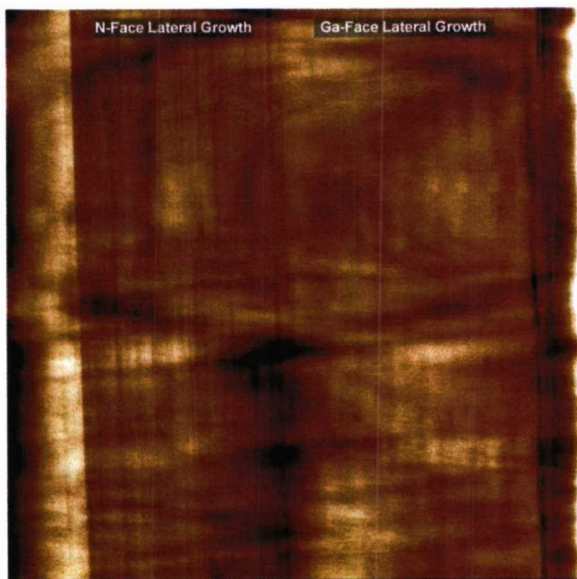


Fig. 14. 25x25  $\mu\text{m}$  AFM scan of a coalesced  $a$ -plane S-LEO film. Vertical lines visible in “N-Face Lateral Growth” region are stacking faults.

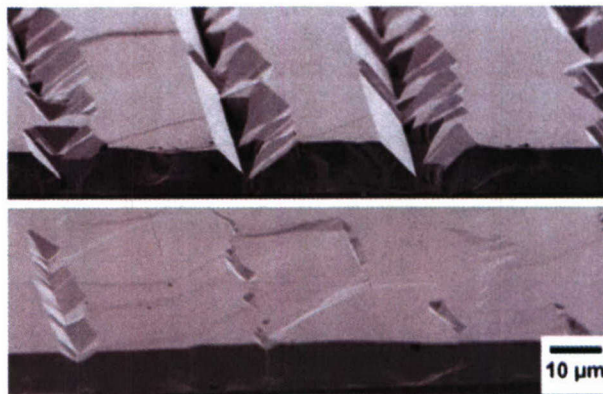
The greatest challenge in using the S-LEO approach for non-polar GaN defect reduction is strain management. Dislocations and surface roughness, two undesirable characteristics of high-quality GaN films, can be beneficial in that they relieve strain in the growing film due to lattice

mismatch. The S-LEO process eliminates these defect structures, thereby removing two means of mitigating grown-in strain. Radii of curvature of the resulting coalesced S-LEO  $a$ -plane GaN films were typically smaller than for standard LEO films, on the order of 1 to 5 m. The residual strain in the S-LEO films often caused cracking of the films on cooling. In order to mitigate this effect, we plan to apply the S-LEO technique to defective free-standing  $m$ -plane and  $a$ -plane GaN films during the Interim Work Effort and Phase II research, eliminating the thermal expansion mismatch problem that is responsible for most of the bowing in S-LEO films.

### ***Spontaneous Delamination via LEO***

In addition to lowering overall extended defect density,  $a$ -plane LEO may also provide a means of obtaining free-standing  $a$ -plane GaN seeds for subsequent boule growth. Unlike  $m$ -plane GaN films, which often self-separate from their  $\text{LiAlO}_2$  substrates to yield free-standing GaN wafers,  $a$ -plane GaN films grown on  $r$ -plane sapphire substrates remain in intimate contact with the substrate. The substrates must be removed by techniques such as lapping or etching, or alternately excimer laser lift-off, during which the GaN-sapphire interface is ablated. However, these approaches are labor intensive and/or have low yield. In our experience, laser lift-off often results in fractured GaN wafer fragments of less than 2-inch diameter. In contrast, we have found that  $a$ -plane LEO GaN, when overgrown from stripes of properly chosen orientation, can self-separate from the substrate during cool-down. Namely, a LEO stripe orientation of  $\langle 1\bar{1}01 \rangle$  ( $43.2^\circ$  from the  $\langle 1\bar{1}00 \rangle$  direction) yields large-area, free-standing  $a$ -plane films. This is apparently due to the high lateral-to-vertical growth ratio that wings on such stripes exhibit. Although the wings on such stripes are often faceted due to the lack of low-index planes parallel to the stripe direction, smooth surfaces were readily achieved upon coalescence, as shown in Fig. 15. During cool-down to room temperature, delamination at the weak wing/mask interface occurred, presumably due to stresses from thermal mismatch between the  $a$ -plane GaN and its underlying sapphire substrate.

Fig. 15. Inclined SEM cross-section micrographs of  $\langle 1\bar{1}01 \rangle$ -oriented  $a$ -plane LEO stripes before (top) and after (bottom) coalescence.



The mechanism for delamination at the wing/mask level is under investigation, but we plan to exploit it as a means of obtaining free-standing  $a$ -plane GaN wafers. One unusual aspect of the separation is that it was only observed when LEO stripes were grown from masks having a period of 20  $\mu\text{m}$  or greater (*e.g.* films grown from a 2/8 mask did not delaminate). However, delamination occurred regardless of film thickness. Films up to  $\sim 40 \mu\text{m}$  thick typically broke apart into many square millimeter-sized flakes. Thicker films fractured into larger fragments with areas on the order of square centimeters. One  $\sim 125 \mu\text{m}$  thick film delaminated largely intact, yielding a free-standing  $a$ -plane GaN wafer having an area equivalent to nearly three-quarters of the original two-inch diameter substrate. Thus in the near future we will focus on

increasing film thickness to increase the mechanical stability of delaminated films to yield full two-inch diameter wafers.

### ***Semi-polar GaN films***

As described above, Inlustra committed the overwhelming majority of its Phase I research effort to non-polar GaN seed film growth development. However, related work on semi-polar GaN film growth was performed at UCSB over the same time period, with contributions by Inlustra researchers. Several key observations were made, including:

- Semi-polar GaN films such as  $\{10\bar{1}3\}$  and  $\{10\bar{1}1\}$  most commonly grow with ‘nitrogen-polar’ free surfaces, as verified by convergent beam electron diffraction<sup>3</sup>. These N-terminated surfaces are disadvantageous for thick film growth, stacking fault generation, and subsequent device re-growth compared to non-polar or Ga-polar (*c*-plane) surfaces.
- ‘Twinning’ domains have been observed in  $\{10\bar{1}3\}$  films on spinel and sapphire substrates if no miscut is employed. Initial substrate miscut control is vital to achieving consistent domain orientation over entire 2-inch wafer surfaces.
- LEO of semi-polar GaN is considerably more challenging than LEO of non-polar or Ga-polar GaN due to the inclination of defects relative to the free surface, and lack of low-index planes normal to the growth plane. Stacking fault elimination is very challenging and threading dislocation elimination requires multiple LEO steps.

Despite these disadvantages, we did investigate thick  $\{11\bar{2}2\}$  GaN films on *m*-plane sapphire briefly, due to the low cost and high quality of the available sapphire substrates. The films exhibited comparable threading dislocation and stacking fault densities to the lowest-quality non-polar GaN films produced in the course of this project. Typical defect densities were on the order of  $5 \times 10^9$  dislocations/cm<sup>2</sup> and  $3 \times 10^5$  basal plane stacking faults/cm. These defects propagated at an inclined angle, dictated by the angle between the semi-polar plane and the *c*-plane and the allowed Burger’s vectors for dislocations in wurtzite crystals. We will likely continue to explore the value of LEO and thick-film growth of semi-polar nitrides as seed films for boule growth.

### ***Remaining Challenges***

Significant progress towards obtaining uniform, low-defect density non-polar GaN substrates was achieved over the course of our Phase I STTR project. However, challenges remain before the thick films produced in this study translate into high-quality boules which can be wafered into uniform, low defect density, and importantly, *low-cost*, non-polar GaN substrates. Among the challenges that will be addressed during the Interim Work and Phase II efforts are:

1. **Improving morphological control of the nucleation phase of S-LEO growth via HVPE of both *a*-plane and *m*-plane GaN.** While S-LEO has been successfully performed utilizing only HVPE as a growth method, more consistent planarization may be achieved when the initial lateral growth, on the order of 500 nm, is performed with MOCVD. Use of MOCVD in this process is a viable but expensive option in producing high-quality non-polar GaN substrates. More simply, additional time must be dedicated to refining the template

processing and initial lateral growth parameters to improve reproducibility in the defect reduction process. S-LEO appears likely to be a much more reproducible and lower-cost approach to non-polar GaN defect reduction than D-LEO, but must be developed further before it is a viable production method.

2. **Stress management in the spontaneous lift-off process for *a*-plane GaN LEO.** We have been able to achieve spontaneous separation of *a*-plane GaN films from *r*-plane sapphire substrates using LEO stripes patterned along the  $\langle 11\bar{0}1 \rangle$  direction. Nearly full two-inch wafers have been obtained by this approach, but the process remains somewhat irreproducible. Refinement of this spontaneous liftoff process will be required to improve wafer yields.
3. **Scale-up of *m*-plane GaN LEO/S-LEO.** It has proven impractical to perform LEO on  $\text{LiAlO}_2$  substrates directly, or on thin GaN films grown upon  $\text{LiAlO}_2$  due to substrate decomposition. Thus all of the *m*-plane GaN LEO work performed to date has been confined to SiC substrates, which offer a good chemical stability at the cost of poor thermal expansion mismatch and small available wafer size. We will solve this problem by first producing thick, free-standing *m*-plane GaN wafers having two-inch diameters, and then perform S-LEO on these wafers to eliminate both the chemical instability of  $\text{LiAlO}_2$  and the thermal mismatch and size constraints of *m*-plane SiC.
4. **Elimination of stacking faults from non-polar GaN.** Threading dislocation reduction is readily achieved in non-polar GaN LEO using virtually any mask geometry. Stacking faults, however, can only be eliminated with masks oriented perpendicular to the *c*-axis. Even then, new faults are generated whenever nitrogen-terminated *c*-planes are exposed. We must further refine our non-polar GaN LEO lateral growth parameters, particularly for *m*-plane LEO, to suppress lateral growth of the N-face wings in favor of rapid growth of Ga-terminated wings. Doing so would reduce the area of the substrate containing stacking faults, but would not eliminate the faults completely. We propose an approach in Section D.2(c) below to address this concern.
5. **Increasing total film thickness while maintaining planar surfaces.** One of the greatest drawbacks to current *c*-plane GaN thick-film or pseudo-boule growth approaches described in the literature is the inability to maintain planar growth fronts after depositing more than  $\sim 1\text{-}3$  mm of material. The work performed during this Phase I STTR project indicated that growth system capacity was the limiting factor in our ability to grow thick non-polar GaN films. We will now port our understanding of planar, non-polar GaN growth to a newly constructed bulk GaN growth system that is designed to operate continuously for weeks rather than hours. Migrating to this larger-capacity growth system while maintaining the planar growth fronts we require for boule growth, will not be without its challenges.

## Conclusion

Inlustra's Phase I STTR research effort on the growth of high-quality, low-defect density GaN thick films yielded promising results for future commercialization of non-polar and semi-polar GaN substrates. The best thick *a*-plane and *m*-plane films had microstructural defect densities and surface roughness values comparable to the best published *c*-plane GaN substrates.

Therefore, the thick non-polar films developed during Phase I and the Interim Work Effort (currently underway) will act as highly suitable seed wafers for bulk GaN boule growth in Phase II. Inlustra's new production-scale bulk GaN growth system, to be brought online during the Interim Work Effort and optimized throughout Phase II, will enable the extended crystal growth periods needed for truly equiaxed GaN boules. In achieving such GaN boule growth, Inlustra will be well positioned to demonstrate cost-effective production of high-quality non-polar and semi-polar GaN substrates.

## REFERENCES

- 
- <sup>1</sup> kSA 'MOS' system, which measures the spacing of multiple laser spots reflected from the wafer surface. See <http://www.k-space.com/Products/MOS.html>.
- <sup>2</sup> B.M. Imer, F. Wu, S.P. DenBaars, and J.S. Speck; *Appl. Phys. Lett.* **88**, 061908 (2006).
- <sup>3</sup> T.J. Baker, B.A. Haskell, F. Wu, J.S. Speck, S. Nakamura; *Japn. J. Appl. Phys.* **45**, L154-57 (2006).

# REPORT OF INVENTIONS AND SUBCONTRACTS

(Pursuant to "Patent Rights" Contract Clause) (See Instructions on back)

Form Approved  
OMB No. 9000-0095  
Expires Jan 31, 2008

The public reporting burden for this collection of information is estimated to average 1 hour per response, including the time for reviewing instructions, searching existing data sources, gathering and maintaining the data needed, and completing and reviewing the collection of information. Send comments regarding this burden estimate or any other aspect of this collection of information, including suggestions for reducing the burden, to the Department of Defense, Executive Services Directorate (9000-0095). Respondents should be aware that notwithstanding any other provision of law, no person shall be subject to any penalty for failing to comply with a collection of information if it does not display a currently valid OMB control number.

## PLEASE DO NOT RETURN YOUR COMPLETED FORM TO THE ABOVE ORGANIZATION. RETURN COMPLETED FORM TO THE CONTRACTING OFFICER.

1. a. NAME OF CONTRACTOR/SUBCONTRACTOR INLUSTRATE TECHNOLOGIES, LLC		c. CONTRACT NUMBER W911NF-06-C-0133		2. a. NAME OF GOVERNMENT PRIME CONTRACTOR US ARMY RDECOM ACQ CTR		c. CONTRACT NUMBER SAME		3. TYPE OF REPORT (X one) a. INTERIM <input type="checkbox"/> b. FINAL <input checked="" type="checkbox"/>	
b. ADDRESS (Include ZIP Code) 5385 HOLLISTER AVE., #113 SANTA BARBARA, CA 93111-2391		d. AWARD DATE (YYYYMMDD) 20060806		b. ADDRESS (Include ZIP Code) 4300 S. MIAMI BLVD. DURHAM, NC 27703		d. AWARD DATE (YYYYMMDD) 20060806		4. REPORTING PERIOD (YYYYMMDD) a. FROM 20060806 b. TO 20070206	

## SECTION I - SUBJECT INVENTIONS


5. "SUBJECT INVENTIONS" REQUIRED TO BE REPORTED BY CONTRACTOR/SUBCONTRACTOR (If "None," so state)		DISCLOSURE NUMBER, PATENT APPLICATION SERIAL NUMBER OR PATENT NUMBER c.		ELECTION TO FILE PATENT APPLICATIONS (X)				CONFIRMATORY INSTRUMENT OR ASSIGNMENT FORWARDED TO CONTRACTING OFFICER (X)	
NAME(S) OF INVENTOR(S) (Last, First, Middle Initial)	TITLE OF INVENTION(S)	b.		(1) UNITED STATES (a) YES (b) NO		(2) FOREIGN (a) YES (b) NO		e.	
N/A	N/A	N/A						(a) YES (b) NO	

f. EMPLOYER OF INVENTOR(S) NOT EMPLOYED BY CONTRACTOR/SUBCONTRACTOR		g. ELECTED FOREIGN COUNTRIES IN WHICH A PATENT APPLICATION WILL BE FILED	
(1) (a) NAME OF INVENTOR (Last, First, Middle Initial) N/A	(2) (a) NAME OF INVENTOR (Last, First, Middle Initial)	(2) FOREIGN COUNTRIES OF PATENT APPLICATION	
(b) NAME OF EMPLOYER	N/A	N/A	
(c) ADDRESS OF EMPLOYER (Include ZIP Code)	N/A		

## SECTION II - SUBCONTRACTS (Containing a "Patent Rights" clause)

6. SUBCONTRACTS AWARDED BY CONTRACTOR/SUBCONTRACTOR (If "None," so state)		FAR "PATENT RIGHTS" d.		DESCRIPTION OF WORK TO BE PERFORMED UNDER SUBCONTRACT(S) e.		SUBCONTRACT DATES (YYYYMMDD) f.	
NAME OF SUBCONTRACTOR(S) a.	ADDRESS (Include ZIP Code) b.	SUBCONTRACT NUMBER(S) c.	(1) CLAUSE NUMBER	(2) DATE (YYYYMM)			(1) AWARD
UNIV. OF CALIFORNIA, SANTA BARBARA	3227 CHEADLE HALL SANTA BARBARA, CA 93105	SB070020	2	200609	PERFORM RESEARCH SUPPORTING CONTRACTOR'S STTR CONTRACT		20060806
							20070206

## SECTION III - CERTIFICATION

7. CERTIFICATION OF REPORT BY CONTRACTOR/SUBCONTRACTOR (Not required if: (X as appropriate))		NONPROFIT ORGANIZATION	
I certify that the reporting party has procedures for prompt identification and timely disclosure of "Subject Inventions," that such procedures have been followed and that all "Subject Inventions" have been reported.		<input checked="" type="checkbox"/> SMALL BUSINESS or	
a. NAME OF AUTHORIZED CONTRACTOR/SUBCONTRACTOR OFFICIAL (Last, First, Middle Initial) FINI, PAUL T.	b. TITLE CHIEF TECHNOLOGY OFFICER	c. SIGNATURE 	
		d. DATE SIGNED 20070307	